13

Adaptive Harmonic IIR Notch Filters for Frequency Estimation and Tracking

Li Tan[1], Jean Jiang[2] and Liangmo Wang[3]
[1,2]*Purdue University North Central*
[3]*Nanjing University of Science and Technology*
[1,2]*USA*
[3]*China*

1. Introduction

In many signal processing applications, adaptive frequency estimation and tracking of noisy narrowband signals is often required in communications, radar, sonar, controls, biomedical signal processing, and the applications such as detection of a noisy sinusoidal signal and cancellation of periodic signals. In order to achieve the objective of frequency tracking and estimation, an adaptive finite impulse response (FIR) filter or an adaptive infinite impulse response (IIR) notch filter is generally applied. Although an adaptive FIR filter has the stability advantage over an adaptive IIR notch filter, it requires a larger number of filter coefficients. In practical situations, an adaptive IIR notch filter (Chicharo & Ng, 1990; Kwan & Martin, 1989; Nehorai, 1985) is preferred due to its less number of filter coefficients and hence less computational complexity. More importantly, a second-order adaptive pole/zero constrained IIR notch filter (Xiao et al, 2001; Zhou & Li, 2004) can effectively be applied to track a single sinusoidal signal. If a signal contains multiple frequency components, then we can estimate and track its frequencies using a higher-order adaptive IIR notch filter constructed by cascading second-order adaptive IIR notch filters (Kwan & Martin, 1989). To ensure the global minimum convergence, the filter algorithm must begin with initial conditions, which require prior knowledge of the signal frequencies.

However, in many practical situations, a sinusoidal signal may be subjected to nonlinear effects (Tan & Jiang, 2009a, 2009b) in which possible harmonic frequency components are generated. For example, the signal acquired from a sensor may undergo saturation through an amplifier. In such an environment, we may want to estimate and track the signal's fundamental frequency as well as any harmonic frequencies. Using a second-order adaptive IIR notch filter to estimate fundamental and harmonic frequencies is insufficient, since it only accommodates one frequency component. On the other hand, applying a higher-order IIR notch filter may not be effective due to adopting multiple adaptive filter coefficients and local minimum convergence of the adaptive algorithm. In addition, monitoring the global minimum using a grid search method requires a huge number of computations, and thus makes the notch filter impractical in real time processing. Therefore, in this chapter, we propose and investigate a novel adaptive harmonic IIR notch filter with a single adaptive coefficient to efficiently perform frequency estimation and tracking in a harmonic frequency environment.

The proposed chapter first reviews the standard structure of a cascaded second-order pole/zero constrained adaptive IIR notch filter and its associated adaptive algorithm. Second, we describe the structure and algorithm for a new adaptive harmonic IIR notch filter under a harmonic noise environment. The key feature is that the proposed filter contains only one adaptive parameter such that its global minimum of the MSE function can easily be monitored during adaptation. For example, when the input fundamental signal frequency has a step change (the signal frequency switches to a different frequency value), the global minimum location of the MSE function is also changed. The traditional cascaded second-order adaptive IIR notch filter may likely converge to local minima due to its slow convergence; and hence an incorrect estimated fundamental frequency value could be obtained. However, with the proposed algorithms, when a possible local minimum is detected, the global minimum can easily be detected and relocated so that adaptive filter parameters can be reset based on the estimated global minimum, which is determined from the computed MSE function.
In this chapter, we perform convergence analysis of the adaptive harmonic IIR notch filter (Tan & Jiang, 2009). Although such an analysis is a very challenging task due to the extremely complicated plain gradient and MSE functions, with reasonable simplifications we are still able to achieve some useful theoretical results such as the convergence upper bound of the adaptive algorithm. Based on convergence analysis, we further propose a new robust algorithm. Finally, we demonstrate simulation results to verify the performance of the proposed adaptive harmonic IIR notch filters.

2. Background on adaptive IIR notch filters

In this section, we will describe frequency tracking and estimation using standard adaptive IIR notch filters and illustrate some issues when we apply them in a harmonic noise environment.

2.1 Adaptive second-order IIR notch filters

Fig. 1 presents a basic block diagram for a second-order adaptive IIR notch filter for estimation of a single sinusoid. As shown in Fig. 1, the input sinusoid with frequency f needed be estimated and tracked is given below:

$$x(n) = A\cos(2\pi fn / f_s + \alpha) + v(n) \tag{1}$$

where A and α are the amplitude and phase angle; and $v(n)$ is a zero-mean Gaussian noise process. f_s and n are the sampling rate and time index, respectively.

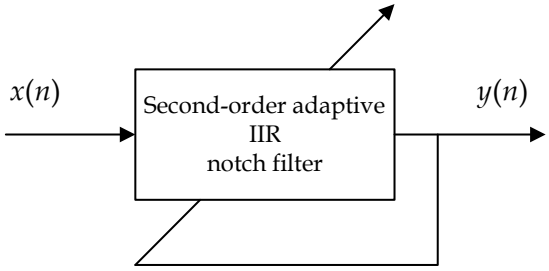

Fig. 1. Second-order adaptive IIR notch filter

To estimate the signal frequency, a standard second-second order adaptive IIR notch filter (Zhou & Li, 2004) is applied with its transfer function given by

$$H(z) = \frac{1 - 2\cos(\theta)z^{-1} + z^{-2}}{1 - 2r\cos(\theta)z^{-1} + r^2 z^{-2}} \tag{2}$$

The transfer function has one notch frequency parameter θ and has zero on the unit circle resulting in an infinite-depth notch. r is the pole radius which controls the notch bandwidth. It requires $0 << r < 1$ for achieving a narrowband notch. Making the parameter θ to be adaptive, that is, $\theta(n)$. The filter output can be expressed as

$$y(n) = x(n) - 2\cos[\theta(n)]x(n-1) + x(n-2) + 2r\cos[\theta(n)]y(n-1) - r^2 y(n-2) \tag{3}$$

Again, when r is close to 1, the 3-dB notch filter bandwidth can be approximated as $BW \approx 2(1-r)$ radians (Tan, 2007). Our objective is to minimize the filter output power $E[y^2(n)]$. Once the output power is minimized, the filter parameter θ will converge to its corresponding frequency f Hz. For a noise free case, the minimized output power should be zero. Note that for frequency tracking, our expected result is the parameter $\theta(n)$ rather than the filtered signal $y(n)$. A least mean square (LMS) algorithm to minimize the instantaneous output power $y^2(n)$ is often used and listed below:

$$\theta(n+1) = \theta(n) - 2\mu y(n)\beta(n) \tag{4}$$

where the gradient function $\beta(n) = \partial y(n) / \partial\theta(n)$ can be derived as following:

$$\beta(n) = 2\sin[\theta(n)]x(n-1) - 2r\sin[\theta(n)]y(n-1) + 2r\cos[\theta(n)]\beta(n-1) - r^2\beta(n-2) \tag{5}$$

and u is the convergence factor which controls the speed of algorithm convergence. Fig. 2 illustrates the behavior of tacking and estimating a sinusoid with its frequency value of 1 kHz at a sampling rate of 8 kHz for a noise free situation. As shown in Fig. 2, the LMS algorithm converges after 2600 iterations. Again, note that the estimated frequency is 1 kHz

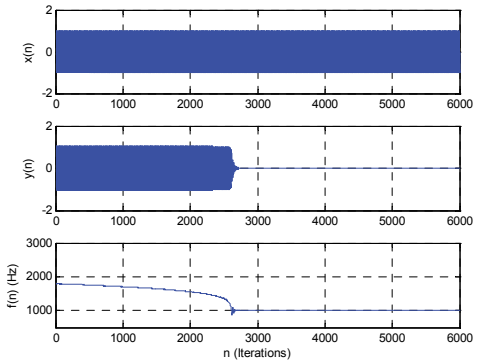

Fig. 2. Frequency tracking of a single sinusoid using a second-order adaptive IIR notch filter (sinusoid: $A = 1$, $f = 1000$ Hz, $f_s = 8000$; adaptive notch filter: $r = 0.95$ and $\mu = 0.005$)

while the filter output approaches to zero. However, when estimating multiple frequencies (or tracking a signal containing not only its fundamental frequency but also its higher-order harmonic frequencies), a higher-order adaptive IIR notch filter using cascading second-order adaptive IIR notch filter is desirable.

2.2 Cascaded higher-order adaptive IIR notch filters

In order to track the fundamental frequency under a harmonic environment, we can cascade second-order IIR notch filters to obtain a higher-order IIR notch filter whose transfer function is yielded as

$$H(z) = \prod_{k=1}^{K} H_k(z) = \prod_{k=1}^{K} \frac{1 - 2\cos\theta_k(n) z^{-1} + z^{-2}}{1 - 2r\cos\theta_k(n) z^{-1} + r^2 z^{-2}} \tag{6}$$

The filter contains K stages (K sub-filters). $\theta_k(n)$ is the adaptive parameter for the kth sub-filter while r is the pole radius as defined in Section 2.1. For an adaptive version, the output from each sub-filter is expressed as

$$y_k(n) = y_{k-1}(n) - 2\cos[\theta_k(n)] y_{k-1}(n-1) + y_{k-1}(n-2) + 2r\cos[\theta_k(n)] y_k(n-1) - r^2 y_k(n-2) \tag{7}$$

Note that the notch filter output $y(n)$ is from the last stage sub-filter, that is, $y(n) = y_K(n)$. After minimizing its instantaneous output power $y_K^2(n)$, we achieve LMS update equations as

$$\theta_k(n+1) = \theta_k(n) - 2 \times 2^{k-1} \mu y_K(n) \beta_{Kk}(n) \tag{8}$$

where $\beta_{Kk}(n)$ is the gradient function which can be determined from the following recursions:

$$\begin{aligned} \beta_{Kk}(n) &= \beta_{(K-1)k}(n) + 2\sin[\theta_k(n)] y_{K-1}(n) - 2\cos[\theta_k(n)] \beta_{(K-1)k}(n-1) \\ &+ \beta_{(K-1)k}(n-2) - 2r\sin[\theta_k(n)] y_{K-1}(n) + 2r\cos[\theta_k(n)] \beta_{Kk}(n-1) - r^2 \beta_{Kk}(n-2) \end{aligned} \tag{9}$$

Fig. 3 shows an example of tracking a signal containing up to its third harmonic components, that is, $\sin(2\pi \times f_a \times n / f_s) + 0.5\cos(2\pi \times 2 f_a \times n / f_s) - 0.25\cos(2\pi \times 3 f_a \times n / f_s)$, where f_a represents the fundamental frequency in Hz and the sampling rate f_s is 8000 Hz. We cascade three second-order adaptive IIR notch filters for this application. For our LMS algorithm, the initial conditions are set to $\theta_1(0) = 2\pi \times 1200 / f_s = 0.3\pi$ radians, $\theta_2(0) = 0.6\pi$ radians, $\theta_3(0) = 0.9\pi$ radians. The fundamental frequency starts from 1225 Hz, and then switches to 1000 Hz and 875 Hz after 10000 iterations and 20000 iterations, respectively. Fig. 3a shows the input and outputs from each filter stage while Fig. 3b displays the tracked frequency values, where $f_1(n) = f_a$, $f_2(n) = 2f_a$ and $f_3(n) = 3f_a$.

With the prior knowledge of the fundamental frequency, the notch filter initially starts from the location nearby the global minimum. The fundamental frequency and harmonic frequencies are tracked with corrected frequency values, that is, 1225, 2x1225, 3x1225 Hz for first 10000 iterations, 1000, 2x1000, 3x1000 Hz from 10001 to 20000 iterations, and 875, 1750,

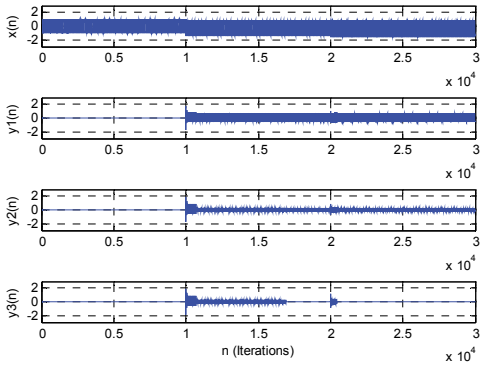

(a)

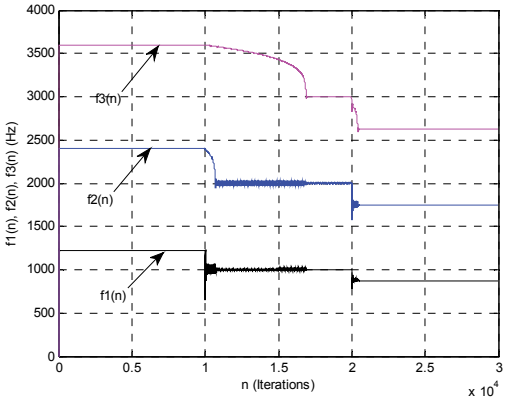

(b)

Fig. 3. Frequency tracking of a signal with its fundamental component, second and third harmonics by using second-order adaptive IIR notch filters in cascade ($r = 0.95$ and $\mu = 0.002$)

2625 Hz from 20001 to 30000 iterations, respectively. We can see that the algorithm exhibits slow convergence when the fundamental frequency switches. Another problem is that the algorithm may converge to a local minimum if it starts at arbitrary initial conditions. As shown in Fig. 4, if the algorithm begins with initial conditions: $\theta_1(0) = 2\pi \times 400 / f_s = 0.1\pi$ radians, $\theta_2(0) = 0.2\pi$ radians, $\theta_2(0) = 0.3\pi$ radians, it converges to local minima with wrong estimated frequencies when the fundamental frequency of the input signal is 1225 Hz. When this fundamental frequency steps to 1000 Hz and 875 Hz, respectively, the algorithm continuously converges to local minima with incorrectly estimated frequency values.

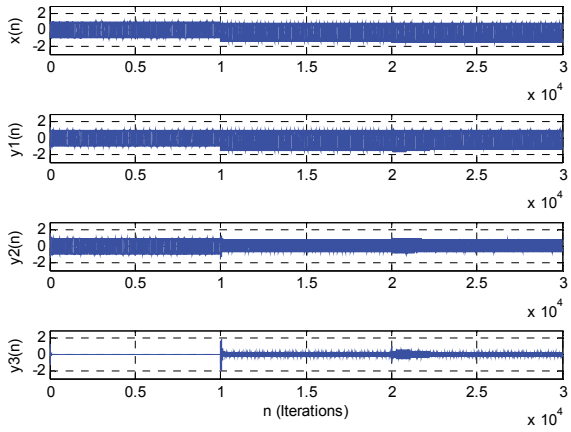

(a)

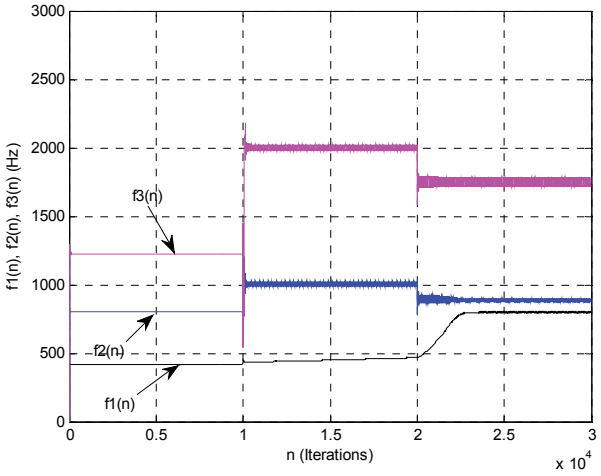

(b)

Fig. 4. Frequency tracking of a single with its fundamental component, second and third harmonics by using second-order adaptive IIR notch filters in cascade

(sinusoid: $A = 1$, $f = 1000$ Hz, $f_s = 8000$; adaptive notch filter: $r = 0.95$ and $\mu = 0.005$).

3. Adaptive harmonic IIR Notch filter structure and algorithm

As described in Section 2.2, a generic higher-order adaptive IIR notch filter suffers from slow convergence and local minimum convergence. To apply the filter successfully, we must have prior knowledge about the frequencies to be tracked. The problem becomes more severe again after the frequencies switch to different values. Using a grid search method to achieve the initial conditions may solve the problem but requires a huge number of computations. However, if we only focus on the fundamental frequency tracking and estimation, this problem can significantly be alleviated.

3.1 Harmonic IIR notch filter structure

Consider a measured signal $x(n)$ containing a fundamental frequency component and its harmonics up to M th order as

$$x(n) = \sum_{m=1}^{M} A_m \cos[2\pi(mf)n / f_s + \alpha_m] + v(n) \tag{10}$$

where A_m, mf, and α_m are the magnitude, frequency (Hz), and phase angle of the m th harmonic component, respectively. To estimate the fundamental frequency in such harmonic frequency environment, we can apply a harmonic IIR notch filter with a structure illustrated in Fig. 5 for the case of $M = 3$ (three harmonics).

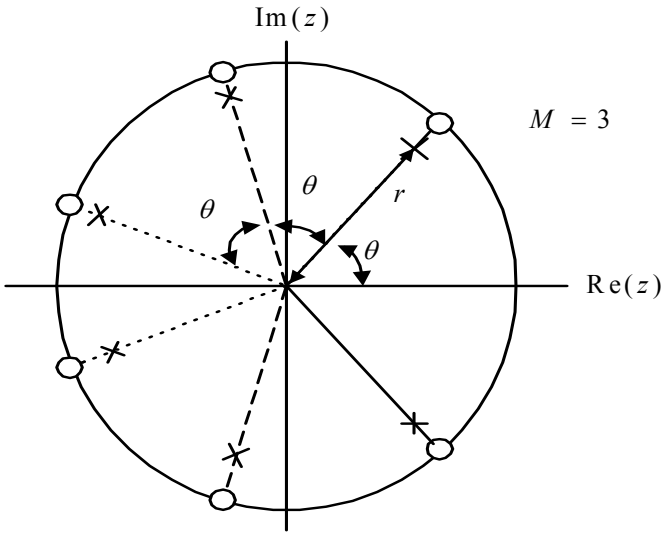

Fig. 5. Pole-zero plot for the harmonic IIR notch filter for $M = 3$

As shown in Fig. 5, to construct a notch filter transfer function, two constrained pole-zero pairs (Nehorai, 1985) with their angles equal to $\pm m\theta$ (multiple of the fundamental frequency angle θ) relative to the horizontal axis are placed on the pole-zero plot for $m = 1, 2, \cdots, M$, respectively. Hence, we can construct M second-order IIR sub-filters. In a cascaded form (Kwan & Martin, 1989), we have

$$H(z) = H_1(z)H_2(z)\cdots H_M(z) = \prod_{m=1}^{M} H_m(z) \tag{11}$$

where $H_m(z)$ denotes the mth second-order IIR sub-filter whose transfer function is defined as

$$H_m(z) = \frac{1 - 2z^{-1}\cos(m\theta) + z^{-2}}{1 - 2rz^{-1}\cos(m\theta) + r^2 z^{-2}} \tag{12}$$

We express the output $y_m(n)$ from the mth sub-filter with an adaptive parameter $\theta(n)$ as

$$y_m(n) = y_{m-1}(n) - 2\cos[m\theta(n)]y_{m-1}(n-1) + y_{m-1}(n-2) + 2r\cos[m\theta(n)]y_m(n-1) - r^2 y_m(n-2) \tag{13}$$

$$m = 1, 2, \cdots, M$$

with $y_0(n) = x(n)$. From (12), the transfer function has only one adaptive parameter $\theta(n)$ and has zeros on the unit circle resulting in infinite-depth notches. Similarly, we require $0 << r < 1$ for achieving narrowband notches. When r is close to 1, its 3-dB notch bandwidth can be approximated by $BW \approx 2(1-r)$ radians. The MSE function at the final stage, $E[y_M^2(n)] = E[e^2(n)]$, is minimized, where $e(n) = y_M(n)$. It is important to notice that once the single adaptive parameter $\theta(n)$ is adapted to the angle corresponding to the fundamental frequency, each $m\theta(n)$ ($m = 2, 3, \cdots, M$) will automatically lock to its harmonic frequency. To examine the convergence property, we write the mean square error (MSE) function (Chicharo & Ng, 1990) below:

$$E\left[e^2(n)\right] = E\left[y_M^2(n)\right] = \frac{1}{2\pi j}\oint \left| \prod_{m=1}^{M} \frac{1 - 2z^{-1}\cos[m\theta(n)] + z^{-2}}{1 - 2rz^{-1}\cos[m\theta(n)] + r^2 z^{-2}} \right|^2 \Phi_{xx} \frac{dz}{z} \tag{14}$$

where Φ_{xx} is the power spectrum of the input signal. Since the MSE function in (14) is a nonlinear function of adaptive parameter θ, it may contain local minima. A closed form solution of (14) is difficult to achieve. However, we can examine the MSE function via a numerical example. Fig. 6 shows the plotted MSE function versus θ for a range from 0 to π / M radians [0 to $f_s / (2M)$ Hz] assuming that all harmonics are within the Nyquist limit for the following conditions: $M = 3$, $r = 0.95$, $f_a = 1000$ Hz, $f_s = 8000$ Hz (sampling rate), signal to noise power ratio (SNR)=22 dB, and 400 filter output samples. Based on Fig. 6, we observe that there exit four (4) local minima in which one (1) global minimum is located at 1 kHz. If we let the adaptation initially start from any point inside the global minimum valley (frequency capture range), the adaptive harmonic IIR notch filter will converge to the global minimum of the MSE error function.

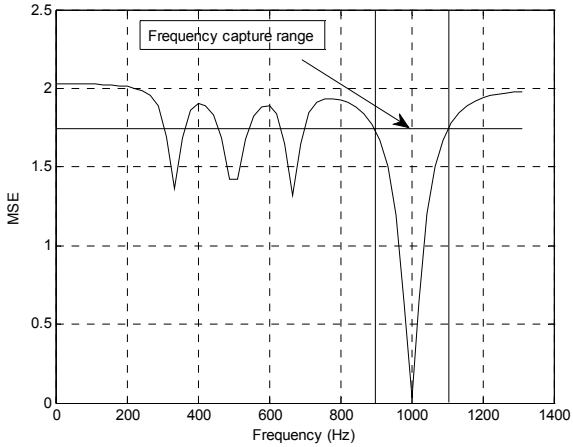

Fig. 6. Error surface of the harmonic IIR notch filter for $M = 3$ and $r = 0.95$

3.2 Adaptive harmonic IIR notch filter algorithms

Similar to Section 2.2, we can derive the LMS algorithm (Tan & Jiang, 2009a, 2009b) by taking the derivative of the instantaneous output power $e^2(n) = y_M^2(n)$ and substituting the result to zero. We achieve

$$\theta(n+1) = \theta(n) - 2\mu y_M(n)\beta_M(n) \tag{15}$$

where the gradient function $\beta_m(n) = \partial y_m(n) / \partial\theta(n)$ is recursively computed as

$$\begin{aligned}\beta_m(n) = \beta_{m-1}(n) - 2\cos[m\theta(n)]\beta_{m-1}(n-1) + 2m\sin[m\theta(n)]y_{m-1}(n-1) + \beta_{m-1}(n-2) \\ + 2r\cos[m\theta(n)]\beta_m(n-1) - r^2\beta_m(n-2) - 2rm\sin[m\theta(n)]y_m(n-1)\end{aligned} \tag{16}$$

$$m = 1, 2, \cdots, M$$

with $\beta_0(n) = \partial y_0(n) / \partial\theta(n) = \partial x(n) / \partial\theta(n) = 0$, $\beta_0(n-1) = \beta_0(n-2) = 0$.

To prevent local minima convergence, the algorithm will start with an optimal initial value θ_0, which is coarsely searched over the frequency range: $\theta = \pi / (180M)$, ..., $179\pi / (180M)$, as follows:

$$\theta_0 = \arg\min_{0<\theta<\pi/M} (E[e^2(n,\theta)]) \tag{17}$$

where the estimated MSE function, $E[e^2(n,\theta)])$, can be determined by using a block of N signal samples:

$$E[e^2(n,\theta)]) \approx \frac{1}{N}\sum_{i=0}^{N-1} y_M^2(n-i,\theta) \tag{18}$$

There are two problems depicted in Fig. 7 as an example. When the fundamental frequency switches from 875 Hz to 1225 Hz, the algorithm starting at the location of 875 Hz on the MSE function corresponding to 1225 Hz will converge to the local minimum at 822 Hz. On the other hand, when the fundamental frequency switches from 1225 Hz to 1000 Hz, the algorithm will suffer a slow convergence rate due to a small gradient value of the MSE function in the neighborhood at the location of 1225 Hz. We will solve the first problem in this section and fix the second problem in next section.

To prevent the problem of local minima convergence due to the change of a fundamental frequency, we monitor the global minimum by comparing a frequency deviation

$$\Delta f = | f(n) - f_0 | \tag{19}$$

with a maximum allowable frequency deviation chosen below:

$$\Delta f_{\max} = 0.5 \times (0.5BW) \tag{20}$$

where $f_0 = 0.5 f_s \theta_0 / \pi$ Hz is the pre-scanned optimal frequency via (17) and (18); BW is the 3-dB bandwidth of the notch filter, which is approximated by $BW = (1-r) f_s / \pi$ in Hz. If

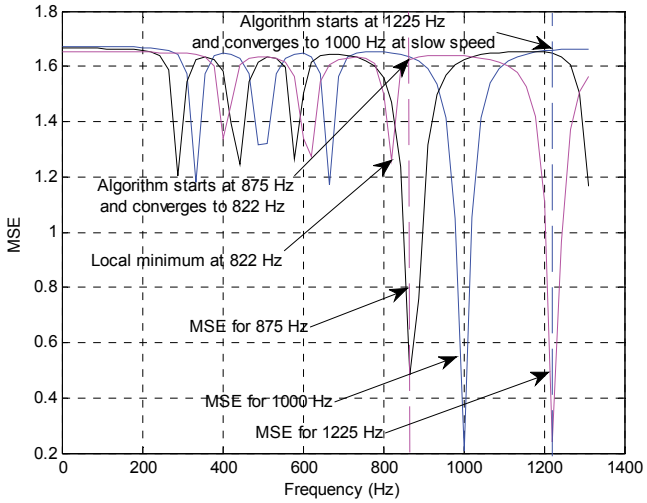

Fig. 7. MSE functions for the fundamental frequencies, 875 Hz, 1000 Hz, and 1225 Hz ($M = 3$, $r = 0.96$, $N = 200$, and $f_s = 8$ kHz)

$\Delta f > \Delta f_{\max}$, the adaptive algorithm may possibly converge to its local minima. Then the adaptive parameter $\theta(n)$ should be reset to its new estimated optimal value θ_0 using (17) and (18) and then the algorithm will resume frequency tracking in the neighborhood of the global minimum. The LMS type algorithm is listed in Table 1.

Step 1: Determine the initial θ_0 using (17) and (18):

Search for $\theta_0 = \arg\min_{0<\theta<\pi/M} E[e^2(n,\theta)]$ for $\theta = \pi/(180M), \cdots, 179\pi/(180M)$

Set the initial condition: $\theta(0) = \theta_0$ and $f_0 = 0.5 f_s \theta_0 / \pi$ Hz

Step 2: Apply the LMS algorithm:

For $m = 1, 2, \cdots, M$

$$y_m(n) = y_{m-1}(n) - 2\cos(m\theta) y_{m-1}(n-1) + y_{m-1}(n-2) + 2r\cos(m\theta) y_m(n-1) - r^2 y_m(n-2)$$

$$\beta_m(n) = \beta_{m-1}(n) - 2\cos[m\theta(n)]\beta_{m-1}(n-1) + 2m\sin[m\theta(n)] y_{m-1}(n-1) + \beta_{m-1}(n-2)$$
$$+ 2r\cos[m\theta(n)]\beta_m(n-1) - r^2\beta_m(n-2) - 2rm\sin[m\theta(n)] y_m(n-1)$$

$$\theta(n+1) = \theta(n) - 2\mu y_M(n)\beta_M(n)$$

Step 3: Convert $\theta(n)$ to the desired estimated fundamental frequency in Hz:

$$f(n) = 0.5 f_s \theta(n) / \pi$$

Step 4: Monitor the global minimum:

if $|f(n) - f_0| > \Delta f_{\max}$, go to step 1

otherwise continue Step 2

Table 1. Adaptive Harmonic IIR notch LMS algorithm

3.3 Convergence performance analysis

We focus on determining a simple and useful upper bound for (15) using the approach in references (Handel & Nehorai, 1994; Petraglia, et al, 1994; Stoica & Nehorai, 1998; Xiao, et al, 2001). For simplicity, we omit the second and higher order terms in the Taylor series expansion of the filter transfer function. We achieve the following results:

$$H(e^{j\omega}, m\theta) \approx H_\omega(m\theta)(\omega - m\theta) \tag{21}$$

where

$$H_\omega(m\theta) = \frac{-2\sin(m\theta)}{(1-r)(e^{jm\theta} - re^{-jm\theta})} \prod_{k=1,k\neq m}^{M} H_k(e^{jm\theta}) = B(m\theta)\angle\phi_m \tag{22}$$

The magnitude and phase of $H_\omega(m\theta)$ in (22) are defined below:

$$B(m\theta) = |H_\omega(m\theta)| \text{ and } \phi_m = \angle H_\omega(m\theta) \tag{23}$$

Considering the input signal $x(n)$ in (10), we now can approximate the harmonic IIR notch filter output as

$$y_M(n) = \sum_{m=1}^{M} mA_m B(m\theta)\cos[(m\theta)n + \alpha_m + \phi_m]\delta_\theta(n) + v_1(n) \tag{24}$$

where $v_1(n)$ is the filter output noise and note that

$$\omega - m\theta = m[\theta(n) - \theta] = m\delta_\theta(n) \tag{25}$$

To derive the gradient filter transfer function defined as $S_M(z) = \beta_M(z) / X(z)$, we obtain the following recursion:

$$S_m(z) = H_m(z)S_{m-1}(z) + \frac{2mz^{-1}\sin(m\theta)[1 - rH_m(z)]}{1 - 2r\cos(m\theta)z^{-1} + r^2z^{-2}} H_1(z)\cdots H_{m-1}(z) \tag{26}$$

Expanding (26) leads to

$$S_M(z) = \sum_{n=1}^{M}\left[\prod_{k=1,k\neq n}^{M} H_k(z)\right]\frac{2\times n\sin(n\theta)z^{-1}}{1 - 2r\cos(n\theta)z^{-1} + r^2z^{-2}} - H(z)\sum_{n=1}^{M}\frac{2r\times n\sin(n\theta)z^{-1}}{1 - 2r\cos(n\theta)z^{-1} + r^2z^{-2}} \tag{27}$$

At the optimal points, $\omega = m\theta$, the first term in (27) is approximately constant, since we can easily verify that these points are essentially the centers of band-pass filters (Petranglia, et al, 1994). The second-term is zero due to $H(e^{jm\theta}) = 0$. Using (22) and (23), we can approximate the gradient filter frequency response at $\omega = m\theta$ as

$$S_M(e^{jm\theta}) = \left[\prod_{k=1,k\neq m}^{M} H_k(e^{jm\theta})\right]\frac{2\times m\sin(m\theta)}{(1-r)(e^{jm\theta} - re^{-jm\theta})} = mB(m\theta)\angle(\phi_m + \pi) \tag{28}$$

Hence, the gradient filter output can be approximated by

$$\beta_M(n) = \sum_{m=1}^{M} mB(m\theta)A_m\cos[(m\theta)n + \alpha_m + \phi_m + \pi] + v_2(n) \tag{29}$$

where $v_2(n)$ is the noise output from the gradient filter. Substituting (24) and (29) in (15) and assuming that the noise processes of $v_1(n)$ and $v_2(n)$ are uncorrelated with the first summation terms in (24) and (29), it leads to the following:

$$E[\delta_\theta(n+1)] = E[\delta_\theta(n)] - E[2\mu y_M(n)\beta_M(n)] \tag{30}$$

$$E[\delta_\theta(n+1)] = E[\delta_\theta(n)] + \mu\sum_{m=1}^{M} m^2A_m^2B^2(m\theta)E[\delta_\theta(n)] - 2\mu E[v_1(n)v_2(n)] \tag{31}$$

$$E[v_1(n)v_2(n)] = \frac{\sigma_v^2}{2\pi j}\oint H(z)S_M(1/z)\frac{dz}{z} \tag{32}$$

where σ_v^2 is the input noise power in (10). To yield a stability bound, it is required that

$$\left|1 + \mu\sum_{m=1}^{M} m^2A_m^2B^2(m\theta)\right| < 1 \tag{33}$$

Then we achieve the stability bound as

$$\mu(\theta) < 2 / \sum_{m=1}^{M} m^2 A_m^2 B^2(m\theta) \tag{34}$$

The last term in (31) is not zero, but we can significantly suppress it by using a varying convergence factor developed later in this section. Since evaluating (34) still requires knowledge of all the harmonic amplitudes, we simplify (34) by assuming that each frequency component has the same amplitude to obtain

$$\mu(\theta) < M / \sigma_x^2 \sum_{m=1}^{M} m^2 B^2(m\theta) \tag{35}$$

where σ_x^2 is the power of the input signal. Practically, for the given M, we can numerically search for the upper bound $\mu_{\max}$ which works for the required frequency range, that is,

$$\mu_{\max} = \min_{0<\theta<\pi/M}[\arg(u(\theta))] \tag{36}$$

Fig. 8 plots the upper bounds based on (36) versus M using $\sigma_x^2 = 1$ for $r = 0.8$, $r = 0.9$, and $r = 0.96$, respectively.

We can see that a smaller upper bound will be required when r and M increase. We can also observe another key feature described in Fig. 9.

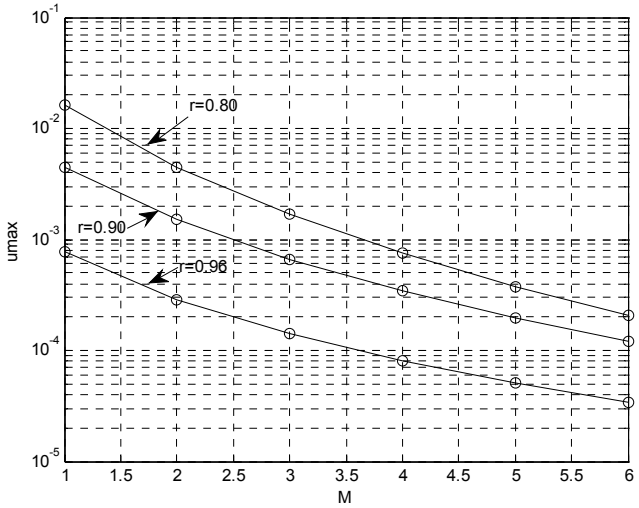

Fig. 8. Plots of the upper bounds in Equation (36) versus M using $\sigma_x^2 = 1$.

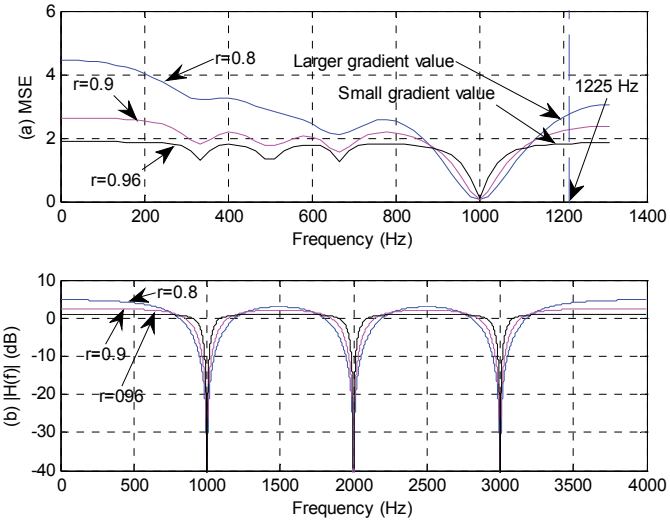

Fig. 9. (a) MSE functions; (b) Magnitude frequency responses ($M = 3$, $N = 200$, $f_s = 8$ kHz)

As shown in Fig. 9, when the pole radius r is much smaller than 1 ($r = 0.8$), we will have a larger MSE function gradient starting at 1225 Hz and then the convergence speed will be increased. But using the smaller r will end up with a degradation of the notch filter frequency response, that is, a larger notch bandwidth. On the other hand, choosing r close to 1 ($r = 0.96$) will maintain a narrow notch bandwidth but result in a slow convergence rate, since the algorithm begins with a small MSE function gradient value at 1225 Hz. Furthermore, we expect that when the algorithm approaches to its global minimum, the cross-correlation $c(n)$ between the final filter output $e(n) = y_M(n)$ and its delayed signal $y_M(n-1)$ becomes uncorrelated, that is, $c(n) = E[y_M(n)y_M(n-1)] \approx 0$. Hence, the cross-correlation measurement can be adopted to control the notch bandwidth and convergence factor. We propose the improved algorithm with varying bandwidth and convergence factor below:

$$c(n) = \lambda c(n) + (1-\lambda) y_M(n) y_M(n-1) \tag{37}$$

$$r(n) = r_{\min} + \Delta r \cdot e^{-\alpha |c(n)|} \tag{38}$$

$$\mu(n) = \mu_{\max}(1 - e^{-\alpha |c(n)|}) \tag{39}$$

where $0 << \lambda < 1$, $r_{\min} < r(n) \le r_{\min} + \Delta r < 1$ with $r_{\min} = 0.8$ (still providing a good notch filter frequency response), $\mu_{\max}$ is the upper bound for $r(n) = r_{\min} + \Delta r$, and α is the damping constant, which controls the speed of change for the notch bandwidth and convergence factor. From (37), (38), and (39), our expectation is as follows: when the algorithm begins to work, the cross-correlation $c(n)$ has a large value due to a fact that the filter output contains fundamental and harmonic signals. The pole radius $r(n)$ in (38) starts with a smaller value to increase the gradient value of the MSE function at the same time the

step size $u(n)$ in (39) changes to a larger value. Considering both factors, the algorithm achieves a fast convergence speed. On the other hand, as $c(n)$ approach to zeroe, $r(n)$ will increases its value to preserve a narrow notch bandwidth while $u(n)$ will decay to zero to reduce a misadjustment as described in (31).
To include (37), (38), and (39) in the improved algorithm, the additional computational complexity over the algorithm proposed in the reference (Tan & Jiang, 2009a, 2009b) for processing each input sample requires six (6) multiplications, four (4) additions, two (2) absolute operations, and one (1) exponential function operation. The new improved algorithm is listed in Table 2.

Step 1: Determine the initial θ_0 using (17) and (18):

Search for $\theta_0 = \underset{0<\theta<\pi/M}{\arg}(\min E[e^2(n,\theta)])$ for $\theta = \pi/(180M),\cdots,179\pi/(180M)$

Set the initial condition: $\theta(0) = \theta_0$ and $f_0 = 0.5 f_s \theta_0 / \pi$ Hz,

$u_{\max}$, $r_{\min}$, λ, α

Step 2: Apply the LMS algorithm:

For $m = 1,2,\cdots,M$

$$y_m(n) = y_{m-1}(n) - 2\cos(m\theta)y_{m-1}(n-1) + y_{m-1}(n-2) + 2r(n)\cos(m\theta)y_m(n-1) - r^2(n)y_m(n-2)$$

$$\beta_m(n) = \beta_{m-1}(n) - 2\cos[m\theta(n)]\beta_{m-1}(n-1) + 2m\sin[m\theta(n)]y_{m-1}(n-1) + \beta_{m-1}(n-2) + 2r(n)\cos[m\theta(n)]\beta_m(n-1) - r^2(n)\beta_m(n-2) - 2r(n)m\sin[m\theta(n)]y_m(n-1)$$

$$c(n) = \lambda c(n) + (1-\lambda)y_M(n)y_M(n-1)$$

$$r(n) = r_{\min} + \Delta r \cdot e^{-\alpha|c(n)|}$$

$$\mu(n) = \mu_{\max}(1 - e^{-\alpha|c(n)|})$$

$$\theta(n+1) = \theta(n) - 2\mu(n)y_M(n)\beta_M(n)$$

Step 3: Convert $\theta(n)$ to the desired estimated fundamental frequency in Hz:

$$f(n) = 0.5 f_s \theta(n) / \pi$$

Step 4: Monitor the global minimum:

if $|f(n) - f_0| > \Delta f_{\max}$, go to step 1

otherwise continue Step 2

Table 2. New adaptive harmonic IIR notch LMS algorithm with varying notch bandwidth and convergence factor

3.4 Simulation results

In our simulations, an input signal containing up to third harmonics is used, that is,

$$x(n) = \sin(2\pi \times f_a \times n / f_s) + 0.5\cos(2\pi \times 2f_a \times n / f_s) - 0.25\cos(2\pi \times 3f_a \times n / f_s) + v(n) \quad (41)$$

where f_a is the fundamental frequency and $f_s = 8000$ Hz. The fundamental frequency changes for every $n = 2000$ samples. Our developed algorithm uses the following parameters:

$$M = 3,\ N = 200,\ \alpha = 10,\ c(0) = 0.2,\ \lambda = 0.997,$$

$$r_{\min} = 0.8\,,\ \Delta r = 0.16$$

The upper bound $\mu_{\max} = 2.14 \times 10^{-4}$ is numerically searched using (35) for $r = 0.96$. The behaviors of the developed algorithm are demonstrated in Figs. 10-13. Fig. 10a shows a plot of the MSE function to locate the initial parameter, $\theta(0) = 2\pi \times 1222 / f_s = 0.3055\pi$ when the fundamental frequency is 1225 Hz. Figs. 10b and 10c show the plots of MSE functions for resetting initial parameters $\theta(0) = 0.25\pi$ and $\theta(0) = 0.22225\pi$ when the fundamental frequency switches to 1000 Hz and then 875 Hz, respectively. Fig. 11 depicts the noisy input signal and each sub-filter output. Figs. 12a to 12c depicts the cross correlation $c(n)$, pole radius $r(n)$, and adaptive step size $\mu(n)$. Fig. 12d shows the tracked fundamental frequencies. As expected, when the algorithm converges, $c(n)$ approaches to zero (uncorrelated), $r(n)$ becomes $r_{\max} = 0.96$ to offer a narrowest notch bandwidth. At the same time, $\mu(n)$ approaches to zero so that the misadjustment can be reduced. In addition, when

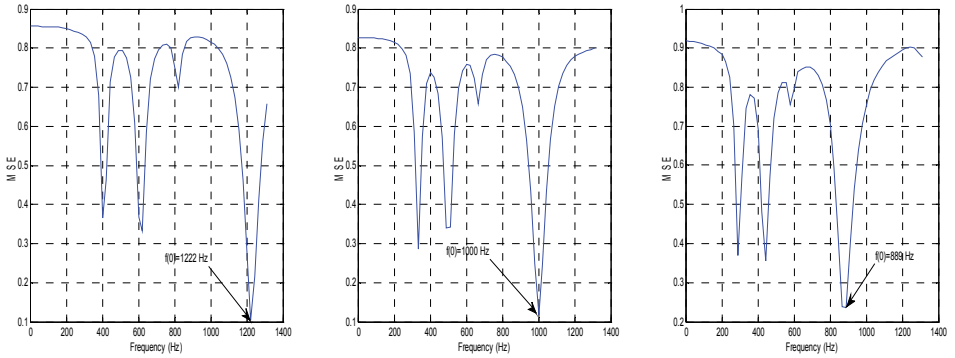

(a) (b) (c)

Fig. 10. Plots of MSE functions for searching the initial adaptive parameter

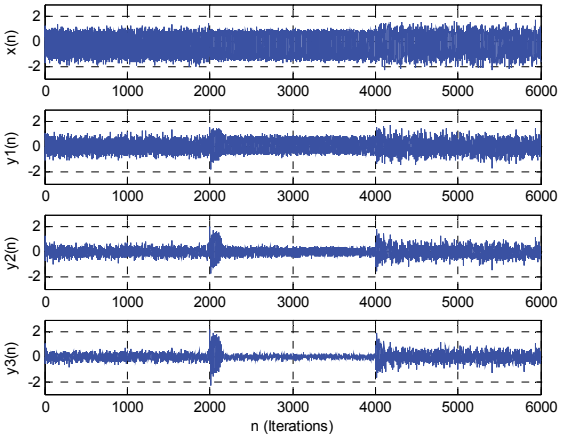

Fig. 11. Input and each sub-filter output for new adaptive harmonic IIR notch filter with varying bandwidth and convergence factor

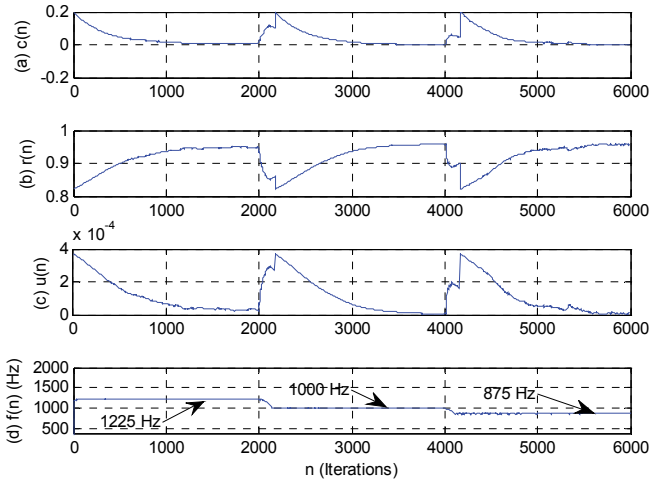

Fig. 12. (a) The cross correlation $c(n)$ between the notch filter output and its delayed output; (b) Varying notch filter parameter $r(n)$; (c) Varying convergence factor $\mu(n)$; (d) Tracked fundamental frequencies $f(n)$.

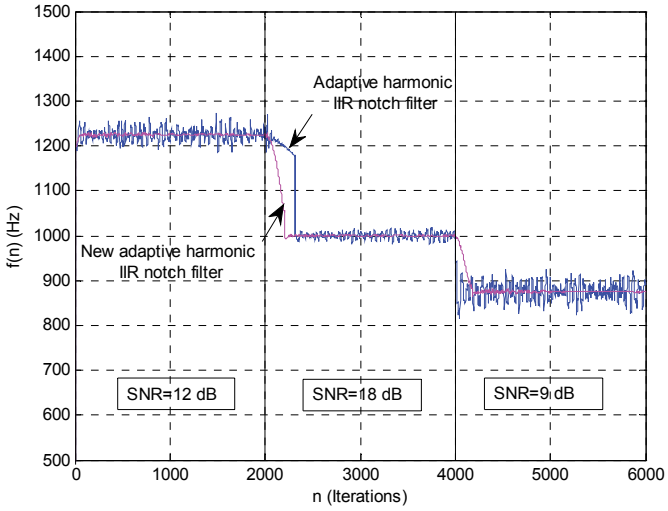

New algorithm: $\mu_{\max} = 2.14 \times 10^{-4}$, $r_{\min} = 0.8$ and $r_{\max} = 0.96$

Algorithm (Tan & Jiang, 2009): $r = 0.96$ and $\mu = 2 \times 10^{-4}$

Fig. 13. Frequency tracking comparisons in the noise environment

the frequency changes from 1225 Hz to 1000 Hz, the algorithm starts moving away from its original global minimum, since the MSE function is changed. Once the tracked frequency is moved beyond the maximum allowable frequency deviation $\Delta f_{\max}$, the algorithm relocates θ_0 and reset $\theta(n) = \theta_0$; and $\theta(n)$ is reset again after the frequency is switched from 1000 Hz to 875 Hz. The improved algorithm successfully tracks the signal fundamental frequency and its changes.

To compare with the algorithm recently proposed in the reference (Tan & Jiang, 2009b), we apply the same input signal to the adaptive harmonic IIR notch filter using a fixed notch bandwidth ($r = 0.96$) and a fixed convergence factor, $\mu = 2.14 \times 10^{-4}$. As shown in Fig. 13, the improved algorithm is much robust to noise under various SNR conditions. This is because when the algorithm converges, the varying convergence factor approaches to zero to offer a smaller misadjustment.

Fig. 14 shows the comparison of standard deviation of the estimated frequency between two algorithms, where we investigate the following condition: $f_a = 1000$ Hz, $M = 3$ using 5000 iterations. For the previous algorithm, we use $r = 0.96$ and $\mu = 10^{-4}$ while for the improved algorithm, all the parameters are the same except that $\mu_{\max} = 10^{-4}$. For each algorithm, we obtain the results using 50 independent runs under each given signal to noise ratio (SNR). From Fig. 14, it is evident that the developed adaptive harmonic IIR notch filter with varying notch bandwidth and convergence factor offers a significant improvement.

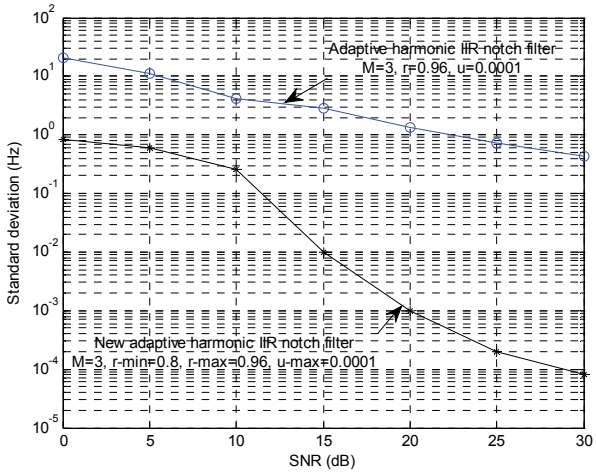

Fig. 14. Tracking error performance of the proposed algorithm

4. Conclusion

In this chapter, we have reviewed the standard adaptive IIR notch filters for applications of single frequency and multiple frequency estimation as well as tracking in the harmonic noise environment. The problems of slow convergence speed and local minima convergence are addressed when applying a higher-order adaptive IIR notch filter for tracking multiple frequencies or harmonic frequencies. We have demonstrated that the adaptive harmonic IIR

notch filter offers an effective solution for frequency estimation and tracking in a harmonic noise environment. In addition, we have derived a simple and useful stability bound for the adaptive harmonic IIR notch filter. In order to achieve the noise robustness and accuracy of frequency tracking in the noisy environment, we have developed an improved adaptive harmonic IIR notch filter with varying notch bandwidth and convergence factor. The developed algorithm is able to prevent its local minima convergence even when the signal fundamental frequency switches in the tracking process.

5. Acknowledgment

This work was supported in part by the Purdue University 2010 Summer Faculty Research Grant, Indiana, USA.

6. References

Nehorai, A. (1985). A Minimal Parameter Adaptive Notch Filter with Constrained Poles and Zeros. *IEEE Trans. Acoust., Speech, Signal Process.*, Vol. 33, No. 4, pp. 983-996, August 1985.

Kwan, T. & Martin, K. (1989). Adaptive Detection and Enhancement of Multiple Sinusoids Using a Cascade IIR Filter. *IEEE Trans Circuits Syst.*, Vol. 36, No. 7, pp. 937-947, July 1989.

Chicharo, J. & Ng, T. (1990). Gradient-based Adaptive IIR Notch Filtering for Frequency Estimation. *IEEE Trans. Acoust., Speech, Signal Process.*, Vol. 38, No. 5, pp. 769-777, May 1990.

Zhou, J. & Li, G. (2004). Plain Gradient-based Direct Frequency Estimation Using Second-order Constrained Adaptive IIR Notch filter. *Electronics Letters*, vol. 40, No. 5, pp. 351-352, March 2004.

Xiao, Y., Takeshita, Y. & Shida, K. (2001). Steady-state Analysis of a Plain Gradient Algorithm for a Second-order Adaptive IIR Notch Filter with Constrained Poles and Zeros. *IEEE Trans. on Circuits and Systems-II: Analog and Digital Signal Processing*, Vol. 48, No. 7, pp 733-740, July 2001.

Tan, L. & Jiang, J. (2009). Novel Adaptive IIR Notch Filter for Frequency Estimation and Tracking. *IEEE Signal Processing Magazine*, Vol. 26, Issue 6, pp. 168-189, November 2009.

Tan, L. & Jiang, J. (2009). Real-Time Frequency Tracking Using Novel Adaptive Harmonic IIR Notch Filter. *the Technology Interface Journal*, Vol. 9, No. 2, Spring 2009

Tan, L. (2007). *Digital Signal Processing: Fundamentals and Applications*. pp. 358-362, ISBN: 978-0-12-374090-8, Elsevier/Academic Press, 2007.

Stoica, P., & Nehorai, A. (1998). Performance Analysis of an Adaptive Notch Filter with Constrained Poles and Zeros. *IEEE Trans. Acoust., Speech, Signal Process.*, Vol. 36, No. 6, pp. 911-919, June 1998.

Handel, P. & Nehorai, A. (1994). Tracking Analysis of an Adaptive Notch Filterwith Constrained Poles and Zeros. *IEEE Trans. Signal Process.*, Vol. 42, No. 2, pp. 281-291, February 1994.

Petraglia, M., Shynk, J. & Mitra, S. (1994). Stability Bounds and Steady-state Coefficient Variance for a Second-order Adaptive IIR Notch Filter. *IEEE Trans. Signal Process.*, Vol. 42, No. 7, pp. 1841-1845, July 1994.

Adaptive Filtering
Edited by Dr Lino Garcia

ISBN 978-953-307-158-9
Hard cover, 398 pages
Publisher InTech
Published online 06, September, 2011
Published in print edition September, 2011

Adaptive filtering is useful in any application where the signals or the modeled system vary over time. The configuration of the system and, in particular, the position where the adaptive processor is placed generate different areas or application fields such as prediction, system identification and modeling, equalization, cancellation of interference, etc., which are very important in many disciplines such as control systems, communications, signal processing, acoustics, voice, sound and image, etc. The book consists of noise and echo cancellation, medical applications, communications systems and others hardly joined by their heterogeneity. Each application is a case study with rigor that shows weakness/strength of the method used, assesses its suitability and suggests new forms and areas of use. The problems are becoming increasingly complex and applications must be adapted to solve them. The adaptive filters have proven to be useful in these environments of multiple input/output, variant-time behaviors, and long and complex transfer functions effectively, but fundamentally they still have to evolve. This book is a demonstration of this and a small illustration of everything that is to come.

How to reference
In order to correctly reference this scholarly work, feel free to copy and paste the following:

Li Tan, Jean Jiang and Liangmo Wang (2011). Adaptive Harmonic IIR Notch Filters for Frequency Estimation and Tracking, Adaptive Filtering, Dr Lino Garcia (Ed.), ISBN: 978-953-307-158-9, InTech, Available from: http://www.intechopen.com/books/adaptive-filtering/adaptive-harmonic-iir-notch-filters-for-frequency-estimation-and-tracking

INTECH
open science | open minds

InTech Europe
University Campus STeP Ri
Slavka Krautzeka 83/A
51000 Rijeka, Croatia
Phone: +385 (51) 770 447
Fax: +385 (51) 686 166
www.intechopen.com

InTech China
Unit 405, Office Block, Hotel Equatorial Shanghai
No.65, Yan An Road (West), Shanghai, 200040, China
中国上海市延安西路65号上海国际贵都大饭店办公楼405单元
Phone: +86-21-62489820
Fax: +86-21-62489821